

mixture was separated on a column (50 g), eluting with petroleum ether/ether (7:3). As the first fraction **6b** (380 mg, 30%) and as the second fraction **4b** (620 mg, 48%) were isolated. Pure analytical samples were obtained by TLC separation. Comparison of the physical data of **4b** and **6b** with those reported in the literature^{3,5b} was in full agreement.

(1,2/3,4)- and (1,3/2,4)-Cyclohexanetetrol (**4a** and **6a**). A mixture of **4b** or **6b** (316 mg, 1 mmol) and 4 N hydrochloric acid (10 mL) was heated at 90 °C for 5 h. Then the solution was concentrated to give an oily product, which crystallized upon addition of ethanol to afford colorless crystals. Recrystallization from methanol gave pure samples whose melting points did not

change. **4a**: 117 mg (77%), mp 215–217 °C (lit.² mp 216 °C, lit.³ mp 209–211 °C). **6a**: 103 mg (70%), mp 185–185.5 °C (lit.^{2,5b} mp 187–188 °C). All physical data were in full agreement with those reported in the literature.

Acknowledgment. We thank Atatürk University for the Financial support (Grant 1986/5) of this work. We also express our thanks to the Department of Chemistry and the firm TÜRK HENKEL (in İstanbul) for partial support and to Mr. Sahmettin Yildiz for technical assistance.

Kinetics of Ionization of Nitromethane and Phenylnitromethane by Amines and Carboxylate Ions in Me₂SO–Water Mixtures. Evidence of Ammonium Ion–Nitronate Ion Hydrogen Bonded Complex Formation in Me₂SO-Rich Solvent Mixtures

Claude F. Bernasconi,* Dahv A. V. Kliner, Amy S. Mullin, and Jiu Xiang Ni

Thimann Laboratories of the University of California, Santa Cruz, California 95064

Received March 15, 1988

Rate constants of ionization of phenylnitromethane in seven amine buffers and six carboxylate buffers and of nitromethane in five amine buffers were determined in 90% Me₂SO–10% water. Similar experiments with a smaller selection of buffers were performed in water, 50% Me₂SO–50% water, and 70% Me₂SO–30% water. Buffer plots with amine buffers in 70% and 90% Me₂SO, but not with carboxylic acid buffers, showed downward curvature, which was attributed to a hydrogen-bonded association complex between the nitronate ion and the protonated amine. Association equilibrium constants for these complexes were determined, and τ values for hydrogen bonding were calculated on the basis of the Hine equation. These τ values ranging from 0.024 to 0.039 are much higher than those for the association between protonated amines and phenoxide ions in water ($\tau = 0.013$, Stahl and Jencks, *J. Am. Chem. Soc.* 1986, 108, 4196), presumably because of reduced hydrogen-bonding stabilization of the nitronate ions by the solvent. Absence of downward curvature in the buffer plots with carboxylic acids is believed to be a consequence of somewhat lower association constants and, more importantly, of competing nitronic acid formation at the low pH values required to study the carboxylic acids. The possibility that the association complex might represent Bordwell's intermediate in the deprotonation of nitroalkanes (BH⁺...CH(R)NO₂) is discussed and rejected. The *intrinsic* rate constants for proton transfer ($k_0 = k_1^B/q = k_{-1}^{BH}/p$ at $\Delta pK + \log p/q = 0$) increase strongly with increasing Me₂SO content of the solvent, but more so when the ionizing base is a carboxylate ion than when it is an amine. This increase is mainly due to a transition state in which solvation of the developing nitronate ion lags behind proton transfer. When the ionizing base is a carboxylate ion, early desolvation of the base adds to the solvent effect on k_0 , but when the ionizing base is an amine, the late solvation of the developing ammonium ion attenuates the solvent effect on k_0 . The Brønsted β values show the familiar increase with increasing Me₂SO content of the solvent, irrespective of buffer type.

The kinetic study of the ionization of nitroalkanes has played a central role in the development of current mechanistic notions about proton transfer at carbon in general.^{1–5} This is because many features that are typical of proton transfer to or from carbon in general manifest themselves more dramatically with nitroalkanes than with other carbon acids.⁶ The most notable characteristics that

distinguish most proton transfers at carbon from such transfers between normal acids and bases are their high intrinsic barriers and the disparity of their Brønsted coefficients ("imbalances"), with α_{CH} (variation of deprotonation rate with pK_a of carbon acid) being larger than β_B (variation of deprotonation rate with pK_a of base).^{1,2,4,7,8} According to current views,⁹ these two features are in large measure related and actually just different manifestations of the same underlying phenomenon, namely, the fact that the development of resonance and solvation of the carbanion lags behind the proton transfer at the transition state.^{1–3,7–10}

New mechanistic insights have come from the quantitative study of solvent effects on rates and equilibria of

(1) Fukuyama, M.; Flanagan, P. W. K.; Williams, F. T.; Frainer, L.; Miller, S. A.; Schechter, H. *J. Am. Chem. Soc.* 1970, 92, 4689.

(2) (a) Bordwell, F. G.; Boyle, W. J., Jr. *J. Am. Chem. Soc.* 1972, 94, 3907. (b) Bordwell, F. G.; Bartmess, J. E.; Hautala, J. A. *J. Org. Chem.* 1978, 43, 3107.

(3) Kresge, A. J. *Can. J. Chem.* 1975, 52, 1897.

(4) Keefe, J. R.; Morey, J.; Palmer, C. A.; Lee, J. C. *J. Am. Chem. Soc.* 1979, 101, 1295.

(5) Cox, E. G.; Gibson, A. *J. Chem. Soc., Chem. Commun.* 1974, 638.

(6) For reviews, see: (a) Eigen, M. *Angew. Chem., Int. Ed. Engl.* 1964, 3, 1. (b) Bell, R. P. *The Proton in Chemistry*, 2nd ed.; Cornell University: Ithaca, NY, 1973. (c) Kresge, A. J. *Chem. Soc. Rev.* 1973, 2, 475. (d) Crooks, J. E. In *Proton Transfer Reactions*; Caldin, E., Gold, V., Eds.; Wiley: New York, 1975; p 153. (e) Hibbert, F. *Compr. Chem. Kinet.* 1977, 8, 97. (f) Bernasconi, C. F. *Pure Appl. Chem.* 1982, 54, 2335.

(7) Bell, R. P.; Grainger, S. *J. Chem. Soc., Perkin Trans. 2* 1976, 1367.

(8) Terrier, F.; Farrell, P. G.; Lelièvre, J.; Chatrousse, A. P. *J. Chem. Soc., Perkin Trans. 2* 1985, 1479.

(9) (a) Bernasconi, C. F. *Tetrahedron* 1985, 41, 3219. (b) Bernasconi, C. F. *Acc. Chem. Res.* 1987, 20, 301.

(10) Pross, A.; Shaik, S. S. *J. Am. Chem. Soc.* 1982, 104, 1129.

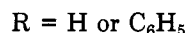
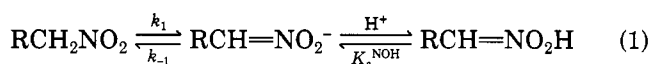
proton transfers. Such studies have recently been reported for the ionization of β -diketones¹¹ and 9-substituted fluorenes¹² in Me₂SO-water mixtures. Since the nitroalkanes show extreme behavior with respect to their high intrinsic barrier and their large imbalances as reflected in large $\alpha_{\text{CH}}-\beta_{\text{B}}$ values, they are also expected to display extreme behavior with respect to solvent effects. This is borne out by the work of Keeffe and co-workers.⁴ In the present paper we report a more systematic solvent-effect study of the ionization of nitromethane and phenylnitromethane in various Me₂SO-water mixtures.¹³

An interesting byproduct of this investigation is our discovery that in Me₂SO-rich solvents there is quite a strong association between the nitronate and ammonium ions. This association is believed to arise from hydrogen bonding of the ammonium ion to the oxygens of the nitronate ion. Even though hydrogen bonding in aqueous solution or partially aqueous media is a phenomenon of considerable importance and interest in a variety of contexts, such as, e.g., acid-base catalysis and the structure of biopolymers in solution, the strength of such associations has only been studied for very few systems.¹⁴ In the present work we were able to determine the association equilibrium constants for several ammonium ion-nitronate ion pairs. Comparison of our results with those recently reported by Stahl and Jencks¹⁴ shows both interesting similarities and differences.

Results

General Features. Proton transfer rates were determined in water and in 50%, 70%, and 90% aqueous Me₂SO by volume at 20 °C. Most measurements were made in amine and carboxylic acid buffers, with a few experiments being conducted in HCl and KOH solutions. Pseudo-first-order conditions, with the nitroalkane as the minor component, were used throughout. The ionic strength was kept constant with KCl (0.5 M in water and 50% Me₂SO, 0.25 M in 70% Me₂SO, and 0.06 M in 90% Me₂SO).

The data in water and 50% Me₂SO can be adequately accounted for by eq 1



with

$$k_1 = k_1^{\text{H}_2\text{O}} + k_1^{\text{OH}} a_{\text{OH}^-} + k_1^{\text{B}} [\text{B}] \quad (2)$$

$$k_{-1} = k_{-1}^{\text{H}} a_{\text{H}^+} + k_{-1}^{\text{H}_2\text{O}} + k_{-1}^{\text{BH}} [\text{BH}] \quad (3)$$

The pseudo-first-order rate constant for equilibrium approach is given by

$$k_{\text{obsd}} = k_1 + k_{-1} \frac{K_a^{\text{NOH}}}{K_a^{\text{NOH}} + a_{\text{H}^+}} \quad (4)$$

The kinetics were followed by approaching the equilibrium either from the nitroalkane side (pH > pK_a^{CH}, with pK_a^{CH} referring to the carbon acid pK_a) or from the ni-

Table I. pK_a^{CH} and pK_a^{NOH} Values for Nitromethane and Phenylnitromethane in Various Me₂SO-Water Mixtures at 20 °C^a

	water	50% Me ₂ SO	70% Me ₂ SO	90% Me ₂ SO
		CH ₃ NO ₂		
pK _a ^{CH}	10.28	11.32	12.44	14.80
pK _a ^{NOH}	3.25 ^b			8.65
[aci]/[nitro]	≈9.3 × 10 ⁻⁸			7.08 × 10 ⁻⁷
K _a ^{CH} /K _a ^{NOH}				
		PhCH ₂ NO ₂		
pK _a ^{CH}	6.77	7.93	8.53 ^c	10.68
pK _a ^{NOH}	3.64 ^d	4.75	5.75	7.73
[aci]/[nitro]	≈7.41 × 10 ⁻⁴	6.61 × 10 ⁻⁴	1.66 × 10 ⁻³	1.12 × 10 ⁻³
K _a ^{CH} /K _a ^{NOH}				

^a μ = 0.5 M in water and 50% Me₂SO, 0.25 M in 70% Me₂SO, and 0.06 M in 90% Me₂SO, all maintained with KCl. ^b 25 °C, ref 19. ^c Reference 13. ^d Average from determinations via eq 8 and 9; pK_a^{NOH} = 3.9 was reported at 25 °C in ref 19.

tronate ion side (pH < pK_a^{CH}). All experiments were performed in a stopped-flow apparatus. When the reaction was conducted in the direction RCH₂NO₂ → RCH=NO₂⁻, it was monitored at λ_{max} of the nitronate ion. When it was conducted in the reverse direction, by mixing an alkaline solution of the nitronate ion with an acidic buffer or HCl, the same wavelength was chosen as long as little nitronic acid was formed in the preequilibrium preceding the conversion of the nitronate ion into the nitroalkane (pH > pK_a^{NOH}). When the pH was substantially lower than pK_a^{NOH} and hence most of the nitronate ion was first converted into the nitronic acid, λ_{max} of this latter was used to monitor the reaction (see Experimental Section).

The results in 70% and 90% Me₂SO with *carboxylic acid* buffers can also be accounted for by eq 1 and 4. However, with *amine* buffers complications arose because of association between the nitronate ions and ammonium ions, as described below.

pK_a^{CH} and pK_a^{NOH} Measurements. Table I summarizes the pK_a^{CH} and pK_a^{NOH} values for nitromethane and phenylnitromethane in the four solvents used in this study. pK_a^{CH} of phenylnitromethane was determined by standard spectrophotometric procedures in all solvents. pK_a^{CH} of nitromethane could be measured by the same method in water and 50% Me₂SO. In 70% and 90% Me₂SO, the use of an indicator method described in the Experimental Section gave more reliable results because of the sluggish response of the glass electrode in strongly alkaline solutions.

pK_a^{NOH} for phenylnitromethane was obtained kinetically in all solvents while pK_a^{NOH} for nitromethane was only measured in 90% Me₂SO (also kinetically), as described below.

Kinetics of Protonation of Phenylnitromethane Anion in Carboxylic Acid Buffers and HCl. We have obtained the following kinetic data. *Water:* HCl (Table II); methoxyacetic acid at pH 3.10, 3.40, 3.70, and 4.00 (Table S1,¹⁵ 20 rate constants); acetic acid at pH 4.31, 4.59, and 4.89 (Table S1,¹⁵ 15 rate constants). *50% Me₂SO-50% water:* methoxyacetic acid at pH 4.23, 4.51, and 4.82 (Table S2,¹⁵ 15 rate constants). *70% Me₂SO-30% water:* methoxyacetic acid at pH 5.32, 5.62, and 5.92 (Table S3,¹⁵ 15 rate constants). *90% Me₂SO-10% water:* dichloroacetic acid at pH 4.20, 4.68, and 5.16 (Table S4,¹⁵ 27 rate constants); cyanoacetic acid at pH 6.25 (Table S4,¹⁵ 12 rate constants).

(15) See paragraph concerning supplementary material at the end of this paper.

(11) (a) Bernasconi, C. F.; Bunnell, R. D. *Isr. J. Chem.* 1985, 26, 420. (b) Bernasconi, C. F.; Paschalis, P. *J. Am. Chem. Soc.* 1986, 108, 2969. (12) (a) Bernasconi, C. F.; Terrier, F. *Can. J. Chem.* 1986, 64, 1273. (b) Bernasconi, C. F.; Terrier, F. *J. Am. Chem. Soc.* 1987, 109, 7115. (13) Preliminary account of this work: Bernasconi, C. F.; Bunnell, R. D.; Klinder, D. A.; Mullin, A.; Paschalis, P.; Terrier, F. *Physical Organic Chemistry 1986*; Kobayashi, M., Ed.; Elsevier: Amsterdam, 1987; p 583. (14) Stahl, N.; Jencks, W. P. *J. Am. Chem. Soc.* 1986, 108, 4196.

Table II. Kinetics of Protonation of Phenylnitromethane Anion in Water at 20 °C^a

buffer	pH	slope, ^b M ⁻¹ s ⁻¹	intercept, ^c s ⁻¹
HCl	1.30		1.21 × 10 ⁻³
	2.00		1.19 × 10 ⁻³
	2.30		1.16 × 10 ⁻³
	2.52		1.14 × 10 ⁻³
	2.80		1.09 × 10 ⁻³
CH ₃ OCH ₂ COOH	3.10	9.10 × 10 ⁻²	9.61 × 10 ⁻⁴
	3.40	1.43 × 10 ⁻¹	7.96 × 10 ⁻⁴
	3.70	2.07 × 10 ⁻¹	6.27 × 10 ⁻⁴
	4.00	2.91 × 10 ⁻¹	3.88 × 10 ⁻⁴
AcOH	4.31	8.86 × 10 ⁻²	2.82 × 10 ⁻⁴
	4.59	1.05 × 10 ⁻¹	1.56 × 10 ⁻⁴
	4.89	1.07 × 10 ⁻¹	9.60 × 10 ⁻⁵

^a μ = 0.5 M (KCl). ^b Slope of plot of k_{obsd} vs [BH], eq 8. ^c Intercept of plot of k_{obsd} vs [BH], eq 6. In HCl, intercept = k_{obsd} .

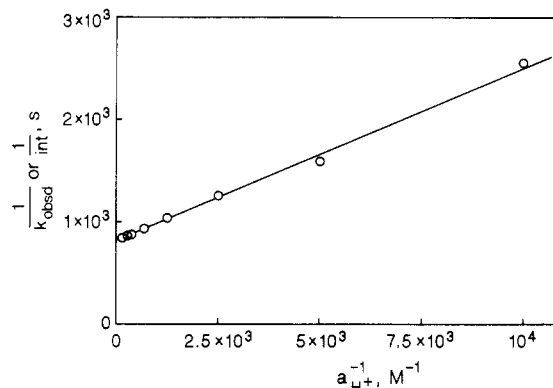
Table III. Kinetics of Protonation of Phenylnitromethane Anion by Carboxylic Acids and H₃O⁺ in Me₂SO-Water Mixtures at 20 °C

buffer	pH	slope, ^a M ⁻¹ s ⁻¹	intercept, ^b s ⁻¹
50% Me ₂ SO-50% Water (v/v) ^c			
CH ₃ OCH ₂ COOH	4.23	1.82	2.91 × 10 ⁻³
	4.51	2.91	2.44 × 10 ⁻³
	4.82	4.34	1.64 × 10 ⁻³
70% Me ₂ SO-30% Water (v/v) ^d			
CH ₃ OCH ₂ COOH	5.32	12.8	e
	5.62	20.0	e
	5.92	28.3	e
90% Me ₂ SO-10% Water (v/v) ^f			
HCl	1.40		8.95 × 10 ⁻⁴
	1.52		9.09 × 10 ⁻⁴
	1.69		8.89 × 10 ⁻⁴
Cl ₂ CHCOOH	4.20	9.96 × 10 ⁻¹	1.89 × 10 ⁻³
	4.68	2.53	e
	5.16	8.95	e
NCCH ₂ COOH	6.25	39.7	e
	6.84	90.9	e
	7.09	88.6	e
CH ₃ OCH ₂ COOH	7.53	174	e
	7.87	309	e
	8.65	352	e
	8.39	247	e
	9.53	122	e

^a Slope of plot of k_{obsd} vs [BH], eq 8. ^b Intercept of plot of k_{obsd} vs [BH], eq 6. In HCl, intercept = k_{obsd} . ^c μ = 0.5 M (KCl). ^d μ = 0.25 M (KCl). ^e Too small to determine. ^f μ = 0.06 M (KCl).

constants); chloroacetic acid at pH 6.84 (Table S4,¹⁵ 12 rate constants); methoxyacetic acid at pH 7.09, 7.53, 7.87, and 8.65 (Table S4,¹⁵ 21 rate constants); β-chloropropionic acid at pH 8.39 (Table S4,¹⁵ 12 rate constants); acetic acid at pH 9.53 (Table S4,¹⁵ 12 rate constants).

Our experiments served three main objectives. The first was to determine the intrinsic rate constant for carboxylic acid protonation of the phenylnitromethane anion/carboxylate ion deprotonation of phenylnitromethane in water and 90% Me₂SO by suitable interpolation or extrapolation of the respective Brønsted plots. The second was to use a large number of such carboxylic acids in 90% Me₂SO in order to examine whether the Brønsted plot might show downward curvature as had been observed in the deprotonation of 1,3-indandione and acetylacetone in Me₂SO-rich media.¹¹ The third objective was to determine pK_a^{NOH} and k_{-1}^{H} in all solvents; since pK_a^{NOH} is close to the pK_a of methoxyacetic acid in all solvents, this was the most extensively used buffer and the only one used in 50% and 70% Me₂SO.

**Figure 1.** Protonation of PhCH=NO₂⁻ by H₃O⁺ in water at 20 °C; plot according to eq 7.

Under most conditions the pH in our experiments was at least 2 units below pK_a^{CH} so that eq 4 simplifies to eq 5. Only in the acetic acid buffer in 90% Me₂SO (pH 9.53,

$$k_{\text{obsd}} = k_{-1} \frac{K_a^{\text{NOH}}}{K_a^{\text{NOH}} + a_{\text{H}^+}} \quad (5)$$

$pK_a^{\text{CH}} = 10.68$) was there a nonnegligible contribution (7%) of the k_1 term to k_{obsd} . At the lower end of the pH range there is further simplification since $k_1^{\text{OH}} a_{\text{OH}^-}$ (eq 2) and $k_{-1}^{\text{H}_2\text{O}}$ (eq 3) are negligible.

Results in Water. Table II summarizes k_{obsd} values in HCl and intercepts (int) and slopes of buffer plots. The intercepts and HCl data obey eq 6. Inversion of eq 6 affords

$$k_{\text{obsd}}(\text{HCl}) \text{ or } \text{int}(\text{buffer}) = k_{-1}^{\text{H}} a_{\text{H}^+} \frac{K_a^{\text{NOH}}}{K_a^{\text{NOH}} + a_{\text{H}^+}} \quad (6)$$

eq 7. A plot according to eq 7 (Figure 1) affords $k_{-1}^{\text{H}} =$

$$\frac{1}{k_{\text{obsd}}(\text{HCl})} \text{ or } \frac{1}{\text{int}(\text{buffer})} = \frac{1}{K_a^{\text{NOH}} k_{-1}^{\text{H}}} + \frac{1}{k_{-1}^{\text{H}} a_{\text{H}^+}} \quad (7)$$

$5.71 \pm 0.20 \text{ M}^{-1} \text{ s}^{-1}$ and $pK_a^{\text{NOH}} = 3.66 \pm 0.02$.

The slopes of the buffer plots are given by eq 8 while a plot of 1/slope vs a_{H^+} (eq 9) yields a straight line from which, in principle, k_{-1}^{BH} and pK_a^{NOH} should be obtainable.

$$\text{slope} = k_{-1}^{\text{BH}} \frac{K_a^{\text{NOH}}}{K_a^{\text{NOH}} + a_{\text{H}^+}} \quad (8)$$

$$\frac{1}{\text{slope}} = \frac{1}{k_{-1}^{\text{BH}}} + \frac{a_{\text{H}^+}}{K_a^{\text{NOH}} k_{-1}^{\text{BH}}} \quad (9)$$

For methoxyacetic acid the plot according to eq 9 (not shown) has both a significant slope and a significant intercept from which one obtains $k_{-1}^{\text{BH}} = (3.89 \pm 0.20) \times 10^{-1} \text{ M}^{-1} \text{ s}^{-1}$ and $pK_a^{\text{NOH}} = 3.62 \pm 0.02$. The latter is in excellent agreement with $pK_a^{\text{NOH}} = 3.66$ determined from eq 8. $k_{-1}^{\text{BH}} = (1.13 \pm 0.05) \times 10^{-1} \text{ M}^{-1} \text{ s}^{-1}$ for acetic acid was obtained by means of eq 10.

$$k_{-1}^{\text{BH}} = \text{slope}(K_a^{\text{NOH}} + a_{\text{H}^+})/a_{\text{H}^+} \quad (10)$$

Results in Me₂SO-Water Mixtures. The slopes and intercepts of the buffer plots are summarized in Table III, along with some data in HCl solution in 90% Me₂SO. In most cases the intercepts were too small to be measured accurately. The analysis of the slopes in the methoxyacetic acid buffers was again by means of eq 9, which yielded k_{-1}^{BH} for methoxyacetic acid and pK_a^{NOH} . k_{-1}^{BH} for the other acids in 90% Me₂SO was obtained via eq 10. k_{-1}^{H} was calculated as $k_{\text{obsd}}/K_a^{\text{NOH}}$ from the experiments in HCl.

Table IV. Kinetics of Reactions of Phenylnitromethane with Amines and KOH in Water and 50% Me₂SO-50% Water at 20 °C^a

buffer	pH	slope, ^b M ⁻¹ s ⁻¹	intercept, ^c s ⁻¹
Water			
morpholine	8.89	8.88 × 10 ⁻¹	
piperidine	11.65	16.2	0.43
KOH		110	~2.0 × 10 ⁻²
50% Me ₂ SO-50% Water			
morpholine	8.68	2.20	
	9.13	2.29	
piperidine	11.05	32.9	
	11.47	36.9	
KOH		1.66 × 10 ³	

^a μ = 0.5 M (KCl). ^b Slope of plot of *k*_{obsd} vs [B] or *a*_{OH}, respectively. ^c Intercept of plot of *k*_{obsd} vs [B] or *a*_{OH}, respectively.

Table V. Kinetics of Reactions of Nitromethane with Amines and KOH in Water and 50% Me₂SO-50% Water at 20 °C^a

buffer	pH	slope, ^b M ⁻¹ s ⁻¹	intercept, ^c s ⁻¹
Water			
morpholine	8.85	1.64	
	8.39	4.72	
piperidine	11.56	2.30	8.20 × 10 ⁻²
KOH		15.3	1.80 × 10 ⁻²
50% Me ₂ SO-50% Water			
morpholine	8.72	82.0	
piperidine	11.02	16.0	
KOH		3.69 × 10 ²	

^a μ = 0.5 M (KCl). ^b Slope of plot of *k*_{obsd} vs [B] or *a*_{OH}, respectively. ^c Intercept of plot of *k*_{obsd} vs [B] or *a*_{OH}, respectively.

Table VI. Rate Constants for Ionization of Nitromethane in Water and in 50% Me₂SO-50% Water at 20 °C^a

B	pK _a ^{BH}	<i>k</i> _{1^B} , M ⁻¹ s ⁻¹	<i>k</i> _{-1^{BH}} , M ⁻¹ s ⁻¹
Water (pK _a ^{CH} = 10.28)			
morpholine	8.90	5.87 × 10 ⁻²	1.41
piperidine	11.55	2.19	1.18 × 10 ⁻¹
OH ⁻	15.64	1.53 × 10 ¹	3.71 × 10 ⁻³ /55.5
50% Me ₂ SO-50% Water (pK _a ^{CH} = 11.32)			
morpholine	8.72	2.06 × 10 ⁻¹	8.20 × 10 ¹
piperidine	11.02	5.42	1.08 × 10 ¹
OH ⁻	17.34	3.69 × 10 ²	9.71 × 10 ⁻³ /27.8

^a μ = 0.5 M (KCl).

The various *k*_{-1^{BH}} and *k*_{-1^H} values, as well as *k*_{1^B} and *k*_{1^{H₂O}} derived therefrom on the basis of the known pK_a^{CH} and pK_a^{BH}, and summarized in Tables VII-IX.

Kinetics of Reactions of Nitromethane and Phenylnitromethane with Amines and KOH. The following data were obtained. *Phenylnitromethane in water*: morpholine at pH 8.89, piperidine at pH 11.56, and KOH (Table S5,¹⁵ 15 rate constants). *Nitromethane in water*: morpholine at pH 8.85 and 8.39, piperidine at pH 11.56, and KOH (Table S6,¹⁵ 20 rate constants). *Phenylnitromethane in 50% Me₂SO-50% water*: morpholine at pH 8.68 and 9.13, piperidine at pH 11.05 and 11.47, and KOH (Table S7,¹⁵ 32 rate constants). *Nitromethane in 50% Me₂SO-50% water*: morpholine at pH 8.72, piperidine at pH 11.02, and KOH (Table S8,¹⁵ 15 rate constants). *Nitromethane in 70% Me₂SO-30% water*: morpholine at pH 8.38, piperidine at pH 10.48 (Table S9,¹⁵ 9 rate constants). *Phenylnitromethane in 90% Me₂SO-10% water*:

Table VII. Rate Constants for the Ionization of Phenylnitromethane in Water and in 50% Me₂SO-50% Water at 20 °C^a

B	pK _a ^{BH}	<i>k</i> _{1^B} , M ⁻¹ s ⁻¹	<i>k</i> _{-1^{BH}} , M ⁻¹ s ⁻¹
Water (pK _a ^{CH} = 6.77, pK _a ^{NOH} = 3.64)			
H ₂ O	-1.74	9.70 × 10 ⁻⁷ /55.5	5.71
CH ₃ OCH ₂ COO ⁻	3.40	1.66 × 10 ⁻⁴	3.89 × 10 ⁻¹
CH ₃ COO ⁻	4.57	7.12 × 10 ⁻⁴	1.13 × 10 ⁻¹
morpholine	8.90	8.88 × 10 ⁻¹	6.53 × 10 ⁻³
piperidine	11.55	1.62 × 10 ¹	2.59 × 10 ⁻⁴
OH ⁻	15.64	1.10 × 10 ²	8.23 × 10 ⁻⁶ /55.5
50% Me ₂ SO-50% Water (pK _a ^{CH} = 7.93, pK _a ^{NOH} = 4.75)			
H ₂ O	-1.44	2.46 × 10 ⁻⁶ /27.8	2.09 × 10 ²
CH ₃ OCH ₂ COO ⁻	4.56	3.40 × 10 ⁻³	7.98
morpholine	8.72	2.01	3.26 × 10 ⁻¹
piperidine	11.02	3.49 × 10 ¹	2.85 × 10 ⁻²
OH ⁻	17.34	~1.7 × 10 ³	~1.8 × 10 ⁻⁵ /27.8

^a μ = 0.5 M (KCl).

Table VIII. Rate Constants and Association Equilibrium Constants for the Ionization of Nitromethane and Phenylnitromethane in 70% Me₂SO-30% Water^a

B	pK _a ^{BH}	<i>k</i> _{1^B} , M ⁻¹ s ⁻¹	<i>k</i> _{-1^{BH}} , M ⁻¹ s ⁻¹	<i>K</i> _{assoc} , M ⁻¹
CH ₃ NO ₂ (pK _a ^{CH} = 12.44)				
morpholine	8.38	2.36 × 10 ⁻¹	2.77 × 10 ³	~6.5
piperidine	10.48	5.06	4.72 × 10 ²	(~6.8)
PhCH ₂ NO ₂ (pK _a ^{CH} = 8.53, pK _a ^{NOH} = 5.75)				
H ₂ O			~2.76 × 10 ³	
CH ₃ OCH ₂ COO ⁻	5.67	6.55 × 10 ⁻²	4.75 × 10 ¹	

^a μ = 0.25 M (KCl).

1-cyanomethylamine at pH 5.94, glycine ethyl ester at pH 7.16 and 9.08, *n*-butylamine at pH 10.96, morpholine at pH 7.91, 8.33, and 8.91, piperidine at pH 10.66, and Dabco at pH 8.85 (Table S10,¹⁵ 104 rate constants). *Nitromethane in 90% Me₂SO-10% water*: morpholine at pH 8.43, piperidine at pH 10.79, 2-methoxyethylamine at pH 8.66, *n*-butylamine at pH 10.94 (Table S11,¹⁵ 30 rate constants).

Results in Water and in 50% Me₂SO-50% Water. Slopes and intercepts of plots of *k*_{obsd} vs [B] or *a*_{OH}, respectively, are summarized in Tables IV and V. Since in these experiments eq 4 simplifies to eq 11, the slopes are

$$k_{\text{obsd}} = k_{1^{\text{OH}}}a_{\text{OH}^-} + k_{-1^{\text{H}_2\text{O}}} + \left[k_{1^{\text{B}}} + k_{-1^{\text{BH}}} \frac{a_{\text{H}^+}}{K_{\text{a}}^{\text{BH}}} \right] [\text{B}] \quad (11)$$

given by (*k*_{1^B} + *k*_{-1^{BH}}*a*_{H⁺}/*K*_a^{BH}) and *k*_{1^{OH}}, respectively, and the intercepts by *k*_{1^{OH}}*a*_{OH⁻} + *k*_{-1^{H₂O}} and *k*_{-1^{H₂O}}, respectively. The various rate constants obtained from our analysis are summarized in Table VI.

Results in 70% and 90% Me₂SO. The bulk of our results pertain to 90% Me₂SO. In contrast to all other experiments reported in this paper, most of the buffer plots displayed significant downward curvature. Figures 2-4 show some representative examples. The curvature is most pronounced for amines with intermediate pK_a values (morpholine, Dabco, 2-methoxyethylamine), and for a given amine, it was stronger with nitromethane than with phenylnitromethane.

The curvature of the buffer plots can be attributed to an association between the nitronate ion and the proton-

Table IX. Rate Constants and Association Equilibrium Constants for the Ionization of Nitromethane and Phenylnitromethane in 90% Me₂SO-10% Water^a

B	pK _a ^{BH}	k ₁ ^B , M ⁻¹ s ⁻¹	k ₋₁ ^{BH} , M ⁻¹ s ⁻¹	K _{assoc} ^c , M ⁻¹	τ ^b
CH ₃ NO ₂ (pK _a ^{CH} = 14.80, pK _a ^{NOH} = 8.65)					
EtOOCCH ₂ NH ₂	8.22	3.68 × 10 ⁻²	1.40 × 10 ⁵	1.13 × 10 ²	0.029
morpholine	8.91	8.52 × 10 ⁻¹	6.62 × 10 ⁵	7.96 × 10 ²	0.039
CH ₃ OCH ₂ CH ₂ NH ₂	10.16	7.47 × 10 ⁻¹	3.26 × 10 ⁴	6.01 × 10 ¹	0.031
piperidine	10.74	9.01	1.03 × 10 ⁵	1.19 × 10 ²	0.037
<i>n</i> -BuNH ₂	10.96	2.92	2.02 × 10 ⁴	4.43 × 10 ¹	0.032
PhCH ₂ NO ₂ (pK _a ^{CH} = 10.68, pK _a ^{NOH} = 7.73)					
H ₂ O	-0.74	9.96 × 10 ⁻⁷ /5.55	4.77 × 10 ⁴		
Cl ₂ CHCOO ⁻	4.68	2.81 × 10 ⁻³	2.81 × 10 ³		
NCCH ₂ COO ⁻	6.25	4.53 × 10 ⁻²	1.22 × 10 ³		
ClCH ₂ COO ⁻	6.84	1.15 × 10 ⁻¹	7.97 × 10 ²		
CH ₃ OCH ₂ COO ⁻	8.17	1.31	4.24 × 10 ²		
ClCH ₂ CH ₂ COO ⁻	8.39	1.55	3.02 × 10 ²		
CH ₃ COO ⁻	9.53	8.78	1.24 × 10 ²		
NCCH ₂ NH ₂	5.94	1.61 × 10 ⁻²	8.83 × 10 ²		
EtOOCCH ₂ NH ₂	8.22	4.78 × 10 ⁻¹	1.38 × 10 ²	9.10 × 10 ¹	0.029
Dabco ^c	8.85	1.28 × 10 ¹	8.68 × 10 ²	3.89 × 10 ¹	0.027
morpholine	8.91	5.52	3.25 × 10 ²	3.54 × 10 ¹	0.027
CH ₃ OCH ₂ CH ₂ NH ₂	10.16	6.89	2.28 × 10 ¹	9.33	0.024
piperidine	10.74	9.95 × 10 ¹	8.67 × 10 ¹		
<i>n</i> -BuNH ₂	10.96	3.60 × 10 ¹	1.89 × 10 ¹	(1.06 × 10 ¹)	(0.027)

^aμ = 0.06 M (KCl). ^bFrom Hine equation, eq 17 (see text). ^cDiazabicyclo[2.2.2]octane.

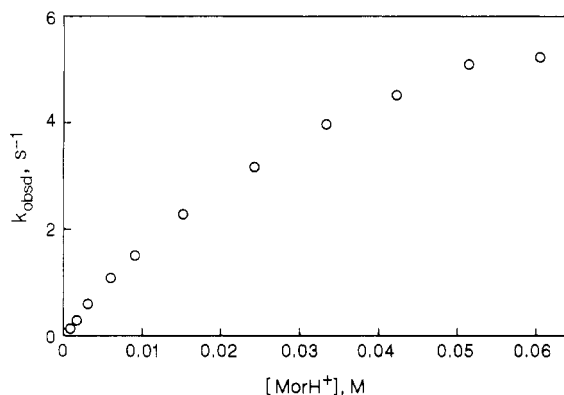
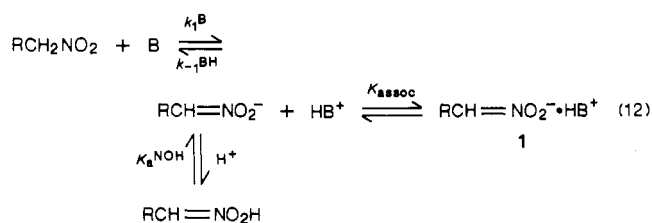


Figure 2. Reaction of PhCH₂NO₂ with a morpholine buffer, [mor]:[morH⁺] = 1:3, pH 8.33 in 90% Me₂SO-10% water at 20 °C; data from Table S10.¹⁵

ated amine, to form a hydrogen-bonded complex such as 1. Inclusion of 1 into the reaction is shown in eq 12. Note



that in eq 12 we have assumed that $k_1 = k_1^{\text{B}}[\text{B}]$ and $k_{-1} = k_{-1}^{\text{BH}}[\text{BH}^+]$, i.e., the other terms in eq 2 and 3 are negligible as is borne out by negligible intercepts in our buffer plots. k_{obsd} for eq 12 is given by eq 13.

$$k_{\text{obsd}} = k_1^{\text{B}}[\text{B}] + \frac{k_{-1}^{\text{BH}}[\text{BH}^+]}{1 + \frac{a_{\text{H}^+}}{K_{\text{aNOH}}} + K_{\text{assoc}}[\text{BH}^+]} \quad (13)$$

On the basis of eq 13 one can rationalize the observed dependence of the degree of curvature on pH, the identity of the buffer, and that of the nitroalkane. Thus, according to eq 13, factors that tend to increase curvature are (a) a pH value that favors the nitroalkane over the nitronate ion since it renders $k_1^{\text{B}}[\text{B}] \ll k_{-1}^{\text{BH}}[\text{BH}^+]$ and makes the

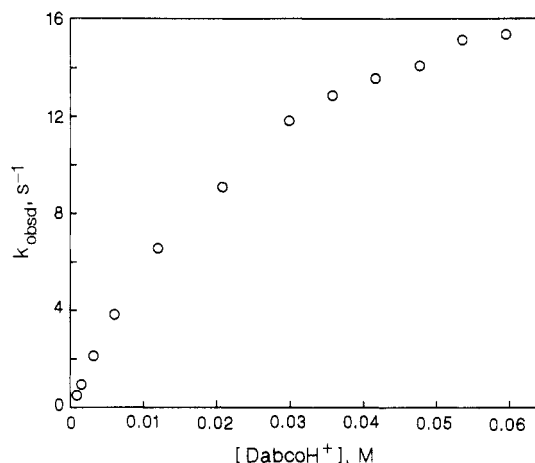


Figure 3. Reaction of PhCH₂NO₂ with a Dabco buffer, [Dabco]:[DabcoH⁺] = 1:1, pH 8.85 in 90% Me₂SO-10% water at 20 °C; data from Table S10.¹⁵

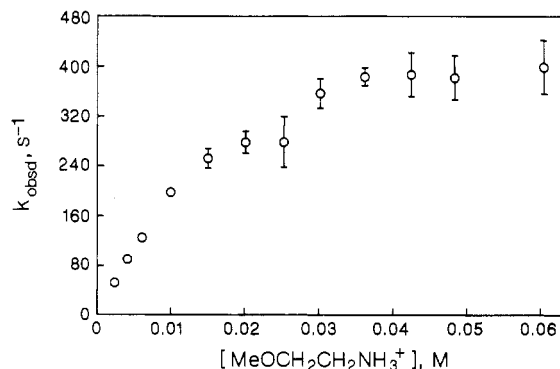


Figure 4. Reaction of CH₃NO₂ with a 2-methoxyethylamine buffer, [B]:[BH⁺] = 1:24, pH 8.66 in 90% Me₂SO-10% water; data from Table S11.¹⁵

second term in eq 13 dominant; (b) a buffer that is more acidic because its hydrogen-bonding strength is enhanced, which should increase K_{assoc} ; (c) a nitronate ion that is more basic since this increases the hydrogen bond acceptor strength and also enhances K_{assoc} . These favorable factors are counteracted by a high pK_a^{NOH} of the aci form and/or

low pH, both of which increase a_{H^+}/K_a^{NOH} in the denominator of the second term of eq 13. This reduces the curvature both by requiring a larger $K_{assoc}[BH^+]$ term for the same reduction in k_{obsd} and by decreasing the size of the entire k_{-1}^{BH} term relative to the k_1^B term in eq 13. Hence the virtual absence of curvature in the reaction of phenylnitromethane ($pK_a^{NOH} = 8.09$) with 1-cyanomethylamine buffer ($pK_a^{BH} = 5.94$) (plot not shown) is accounted for by a large a_{H^+}/K_a^{NOH} term, while in the reaction of piperidine ($pK_a^{BH} = 10.74$) with phenylnitromethane ($pK_a^{CH} = 10.68$) the curvature is hardly detectable because K_{assoc} is small and the $k_1^B[B]$ term contributes significantly to k_{obsd} . The stronger curvature in the reactions of *n*-butylamine and 2-methoxyethylamine with nitromethane compared to the reactions of the same amines with phenylnitromethane must be due to the higher basicity and hence higher K_{assoc} of the nitromethane anion. For the same reason one would expect a stronger curvature for the reaction of morpholine with nitromethane than with phenylnitromethane. However, the rates of the nitromethane reaction were too fast for the stopped-flow method at morpholine concentrations high enough to see curvature, and hence curvature was only detected in the reaction of morpholine with phenylnitromethane.

Finally, the fact that among all amines the curvature is strongest with morpholine ($pK_a^{BH} = 8.91$) and Dabco ($pK_a^{BH} = 8.85$) can be traced to the intermediate range of their pK_a^{BH} values which are low enough to make K_{assoc} large but not so low as to lead to a large a_{H^+}/K_a^{NOH} term.

Quantitative analysis of our data according to eq 13 allowed determination of k_1^B , k_{-1}^{BH} , K_a^{NOH} , and K_{assoc} as follows. For the initial linear part of the buffer plot, eq 13 simplifies to eq 14. In most cases the $k_1^B[B]$ term was

$$k_{obsd} = k_1^B[B] + \frac{k_{-1}^{BH}[BH^+]}{1 + a_{H^+}/K_a^{NOH}} \quad (14)$$

negligible because $pH \ll pK_a^{CH}$ (for all buffers with nitromethane and for morpholine, Dabco, glycine ethyl ester, and 1-cyanomethylamine with phenylnitromethane), and hence the initial slope of a plot of k_{obsd} vs $[BH^+]$ is approximated by eq 8. Analysis according to eq 9 affords k_{-1}^{BH} , or both k_{-1}^{BH} and K_a^{NOH} , depending on the pH range. In those cases where the $k_1^B[B]$ term was not negligible (phenylnitromethane with *n*-butylamine, 2-methoxyethylamine, and piperidine), eq 9 was used to obtain a first approximation of k_{-1}^{BH} , K_a^{NOH} , and k_1^B (from $k_1^B = k_{-1}^{BH}K_a^{CH}/K_a^{BH}$). A second inversion plot according to eq 15 then yielded a second approximation of k_{-1}^{BH} ,

$$\frac{[BH^+]}{k_{obsd} - k_1^B[B]} = \frac{1}{k_{-1}^{BH}} + \frac{a_{H^+}}{k_{-1}^{BH}K_a^{NOH}} \quad (15)$$

K_a^{NOH} , and k_1^B . The iteration was continued until convergence occurred.

K_{assoc} was obtained after rearranging eq 13 to eq 16 and

$$\frac{1}{k_{obsd} - k_1^B[B]} = \frac{1 + \frac{a_{H^+}}{K_a^{NOH}}}{k_{-1}^{BH}[BH]} + \frac{K_{assoc}}{k_{-1}^{BH}} \quad (16)$$

plotting the left-hand side of eq 16 vs $[BH]^{-1}$. K_{assoc} was determined from the intercept of this plot and the known k_{-1}^{BH} .

Table VIII summarizes the results of this analysis in 70% Me₂SO, Table IX those in 90% Me₂SO.

Reaction of 1-Chloro-2,4-dinitrobenzene with *n*-Butylamine and Morpholine in 90% Me₂SO-10% Water. In order to test whether the downward curvature

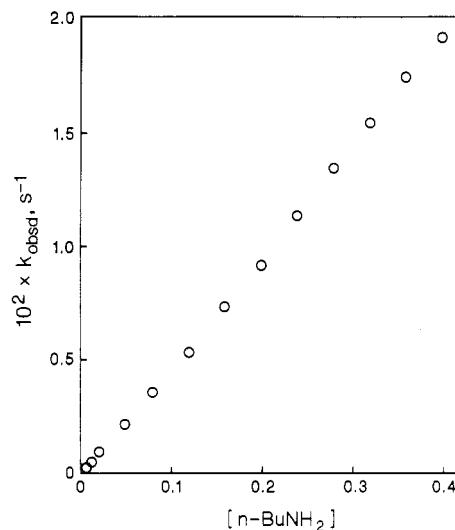


Figure 5. Reaction of 1-chloro-2,4-dinitrobenzene with a *n*-butylamine buffer, [B]:[BH⁺] = 1:1, pH 10.90 in 90% Me₂SO-10% water at 20 °C; data from Table S12.¹⁵

in the plots of k_{obsd} vs $[RR'NH_2^+]$ might be due, completely or in part, to an association of the amines (e.g., $RR'NH_2^+ \cdot HNRR'$), we studied the kinetics of the title reactions under the conditions that had led to the curvature in the reactions with the anions of nitromethane and phenylnitromethane. The results of two series of experiments with morpholine at buffer ratios [B]:[BH⁺] = 1:1 and 1:3 and two similar series with *n*-butylamine are summarized in Table S12¹⁵ (54 rate constants). In all cases strictly linear dependences of k_{obsd} on amine concentration were observed, as shown for a representative example in Figure 5.

Discussion

Solvent Effects on pK_a^{CH} and pK_a^{NOH} . pK_a^{CH} and pK_a^{NOH} values, as well as the ratios of the aci form (nitronic acid) over the nitro form, equivalent to K_a^{CH}/K_a^{NOH} , are summarized in Table I. The following trends are noted.

(1) Both pK_a^{CH} and pK_a^{NOH} increase with increasing Me₂SO content of the solvent; in pure Me₂SO the pK_a values are higher still: $pK_a^{CH} = 17.2$ for CH₃NO₂,¹⁶ $pK_a^{CH} = 12.32$ for PhCH₂NO₂.¹⁷ These strong solvent effects, which are a well-known phenomenon with acids whose conjugate base has the negative charge largely localized on oxygen, are commonly attributed to the decreased hydrogen-bonding solvation of the nitronate ion. This is borne out by a more detailed recent analysis¹⁸ based on free energies of transfer of nitronate ions from water to Me₂SO-water mixtures.

(2) The difference between pK_a^{CH} and pK_a^{NOH} is much smaller for phenylnitromethane than for nitromethane, and hence the percentage of nitronic acid present at equilibrium is much higher for phenylnitromethane than for nitromethane. This result agrees with the generally observed pattern that shows a decrease in K_a^{NOH}/K_a^{CH} as the acidity increases.¹⁹ A specific factor that may play a role in the dramatic enhancement of the aci:nitro ratio by the phenyl group is the possibility of resonance stabilization of the aci form, **2b**. A similar though less dra-

(16) Olmstead, W. N.; Bordwell, F. G. *J. Org. Chem.* **1980**, *45*, 3299.

(17) Bordwell, F. G.; widely circulated list of pK_a values.

(18) Bernasconi, C. F.; Bunnell, R. D. *J. Am. Chem. Soc.* **1988**, *110*, 2900.

(19) Nielsen, A. T. In *The Chemistry of the Nitro and Nitroso Groups*; Feuer, H., Ed.; Wiley: New York, 1969; Part 1, p 349.

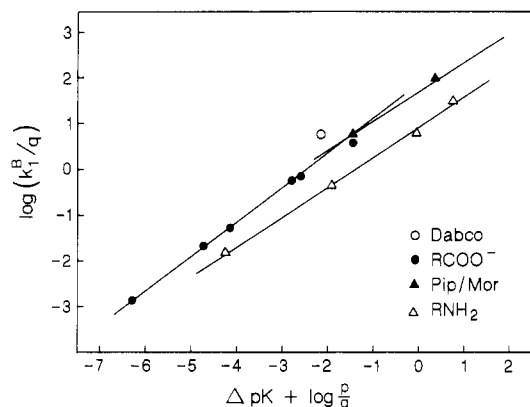
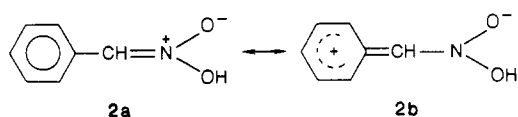
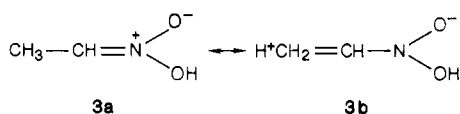


Figure 6. Brønsted plots for the deprotonation of PhCH_2NO_2 by various bases in 90% Me_2SO -10% water at 20 °C.



matic increase in the aci:nitro ratio is seen for nitroethane and 2-nitropropane relative to nitromethane,¹⁹ which may possibly be attributed to hyperconjugative stabilization of the aci form (**3b**); hyperconjugative stabilization of the



nitronate ion of nitroethane and 2-nitropropane has been invoked to explain why the $\text{p}K_a^{\text{CH}}$ of these two compounds is lower than that of nitromethane.^{3,20}

Brønsted Plots. Figure 6 shows Brønsted plots for the deprotonation of phenylnitromethane by carboxylate ions, primary amines, and the piperidine/morpholine pair in 90% Me_2SO -10% water. These plots, as well as the Brønsted plots (not shown) in the other solvents and those for nitromethane, show qualitative and quantitative features that are quite similar to those found in the deprotonation of acetylacetone and 1,3-indandione in the same solvents.¹¹ For example, the Brønsted β value for the carboxylate ions is larger than that for the amines, both in 90% Me_2SO and in water (Table X), and the rate constants for the secondary amines are larger than for the primary amines for a given $\Delta\text{p}K + \log p/q$ (Figure 6). This latter effect as well as the greater reactivity of the tertiary amine Dabco (Figure 6) is a well-known phenomenon that has been explained by the fact that the solvation of ammonium ions decreases in the order $\text{RNH}_3^+ > \text{RR}'\text{NH}_2^+ > \text{RR}'\text{R}'\text{NH}^+$, coupled with late development of this solvation along the reaction coordinate.^{8,11,21}

There may be some slight downward curvature in the plot for the carboxylate ions, as suggested by the way the straight line has been drawn in Figure 6. However, this curvature is substantially less pronounced than that reported for the reactions of acetylacetone^{11a} and 1,3-indandione^{11b} in the same solvent and, in fact, not large enough to be considered established.

The curvature in the previously reported reactions was attributed to a stronger solvation of the more basic carboxylate ions, coupled with the assumption that the loss

Table X. Brønsted β Values^a

% Me_2SO	RCOO^-	RNH_2	pip/mor
CH_3NO_2			
0			0.59
50			0.62
70			0.63
90			0.69
PhCH_2NO_2			
0	0.54		0.48
50			0.52
90	0.75 ^b	0.65	0.69

^a Estimated uncertainty in β values is ± 0.02 to ± 0.03 . ^b Based on the three least basic buffers (see text). If all carboxylate ions are included on the Brønsted line, $\beta = 0.72$.

of this solvation is ahead of proton transfer at the transition state. Since it seemed reasonable to expect that this effect should not depend strongly on the identity of the carbon acid,^{11b} it is somewhat surprising that the curvature in the Brønsted plot for phenylnitromethane is so small. A possible contributing factor to this apparent inconsistency is that the rate constants for the more acidic buffers suffer from a larger than usual experimental uncertainty because they are derived from experiments in which the preequilibrium formation of the aci form contributes in varying degrees to the rate expression (eq 9 and 10), thereby introducing an additional source of potential error. In fact, an increase in $\text{p}K_a^{\text{NOH}}$ by as little as 0.3 log units would induce a significant increase in the curvature of the Brønsted plot.

The Brønsted β values tend to increase in the Me_2SO -richer solvents irrespective of buffer type. A similar trend has been observed in the deprotonation of acetylacetone^{11a} and 1,3-indandione.^{11b} A possible explanation in terms of a larger solvent effect on the stability of the carboxylate ions with increasing $\text{p}K_a^{\text{BH}}$, and a larger solvent effect on the stability of the protonated amines with decreasing $\text{p}K_a^{\text{BH}}$, has been discussed in detail in a previous report.^{11b}

The points for $\text{B} = \text{OH}^-$ and $\text{B} = \text{H}_2\text{O}$ show the following negative deviations from the phenylnitromethane Brønsted plots. In water OH^- deviates by 0.79 log units from the plot defined by the carboxylate ions while the H_2O point deviates by 2.68 log units from the plot defined by piperidine and morpholine. In 50% Me_2SO the H_2O point deviates by 1.72 from the piperidine/morpholine plot; in 90% Me_2SO the same deviation is only 0.29 log units. The negative deviations for OH^- and H_2O are a general phenomenon^{6c} that has been attributed to the particularly strong solvation of OH^- and H_3O^+ , respectively. A possible interpretation as to why these deviations are solvent dependent which is related to the solvent dependence of the Brønsted β values has been discussed in a previous paper.^{11b}

Intrinsic Rate Constants. Intrinsic rate constants, obtained from Brønsted plots as $k_0 = k_1^{\text{B}}/q$ when $\Delta\text{p}K + \log p/q = 0$, are summarized in Table XI. They show the following trends: (1) $\log k_0$ increases with increasing Me_2SO content of the solvent; (2) this increase is more pronounced when the deprotonation is effected by a carboxylate ion instead of an amine; e.g., with phenylnitromethane the change from water to 90% Me_2SO induces a $\Delta \log k_0$ of 3.98 when $\text{B} = \text{RCOO}^-$ and of 2.97 when B is the piperidine/morpholine pair; (3) the solvent effect on k_0 is greater for nitromethane ($\Delta \log k_0 = 3.65$ for $\text{H}_2\text{O} \rightarrow 90\% \text{Me}_2\text{SO}$) than for phenylnitromethane ($\Delta \log k_0 = 2.99$ for $\text{H}_2\text{O} \rightarrow 90\% \text{Me}_2\text{SO}$).

These trends can be largely understood in terms of nonsynchronous solvation/desolvation effects of the ions involved in the reaction, as described in more detail else-

(20) Cardwell, H. M. E. *J. Chem. Soc.* 1951, 2442.

(21) (a) Reference 6b, Chapter 10. (b) Jencks, W. P. *Catalysis in Chemistry and Enzymology*; McGraw-Hill: New York, 1968; p 178. (c) Bernasconi, C. F.; Hibdon, S. A. *J. Am. Chem. Soc.* 1983, 105, 4343.

Table XI. Intrinsic Rate Constants, log *k*₀^a

% Me ₂ SO	RCOO ⁻	RNH ₂	pip/mor
	CH ₃ NO ₂		
0			-0.59
50			0.73
70			1.76
90		2.77	3.06
	PhCH ₂ NO ₂		
0	-2.10		-1.22
50	~-0.57 ^b		-0.25
90	1.88	0.97	1.75

^a Estimated error limits are ±0.05 to ±0.1. ^b Based on *k*₁^B for CH₃OCH₂COO⁻ and an estimated β = 0.6.

where.^{9,12b,22} For example, the hydrogen-bonding solvation of the nitronate ion has a depressing effect on *k*₀ because this solvation develops late along the reaction coordinate. Since this solvation is the strongest in the most aqueous solvents, these are the solvents where *k*₀ is depressed the most. Hence the increase in *k*₀ upon addition of Me₂SO can be understood as a lessening of this depressing effect. Since the hydrogen-bonding solvation of the nitronate ion derived from nitromethane is stronger than that derived from phenylnitromethane¹⁸ and thus has a greater depressing effect on *k*₀, the solvent effect on *k*₀ for nitromethane is larger.

For the reactions involving carboxylate ions as the base, the early desolvation of these ions has a depressing effect on *k*₀ similar to that of the late solvation of the nitronate ions. Again this effect becomes less pronounced in Me₂SO-rich solvents and hence also contributes to the increase in *k*₀ when Me₂SO is added to the solvent. On the other hand, in the reactions involving amine bases the late solvation of the developing ammonium ions leads to a decrease in *k*₀ with increasing Me₂SO content because Me₂SO is a better solvator of the ammonium ion than water. This explains why the solvent effect on *k*₀ for the carboxylate ion promoted ionizations is larger than for the amine-promoted reactions: in the former both the late solvation of the nitronate ion and the early desolvation of the carboxylate ion affect *k*₀ in the same direction; in the latter the effect of late solvation of the ammonium ion counteracts that of the late solvation of the nitronate ion.

Our qualitative conclusions are similar to the ones reached in studying the solvent effect on *k*₀ for the ionization of acetylacetone,^{11a} 1,3-indandione,^{11b} 9-cyano-fluorene, and 9-carbomethoxyfluorene,¹² but quantitatively the solvent effects observed for the nitroalkanes are larger than those for the diketones and especially those for the fluorenes. A semiquantitative analysis of these effects shows that the differences among the various carbon acids can be mainly attributed to large differences in the transfer energies of the various carbanions.^{12b,18} This semiquantitative analysis also suggests that a dynamic solvent may be a contributing factor to the enhancement of *k*₀ in the Me₂SO-rich solvents.^{12b}

Association between Nitronate and Ammonium Ions. In the Results section it was shown that the downward curvature of the plots of *k*_{obsd} vs ammonium ion concentration (Figures 2-4) must be due to a hydrogen-bonding association between the nitronate and the ammonium ion. This conclusion is supported by the following observations: (1) the linearity of the plots of *k*_{obsd} vs amine concentration for the reaction of 1-chloro-2,4-dinitrobenzene with *n*-butylamine and 2-methoxyethylamine

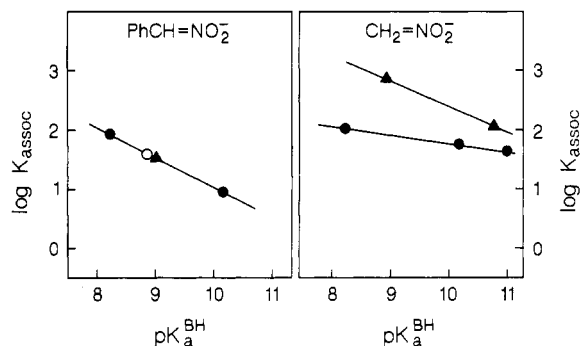
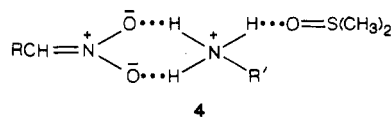


Figure 7. Plots of log *K*_{assoc} vs p*K*_a^{BH} in 90% Me₂SO-10% water at 20 °C; (●) primary ammonium ions, (▲) secondary amines, (○) Dabco.

demonstrates that the curvature cannot be caused by self-association of the amine or the formation of RR'NH₂⁺·HNRR' complexes; (2) the degree of curvature depends in a qualitatively predictable way on the parameters in eq 13 as elaborated upon in the Results section.

By and large, the quantitative dependence of *K*_{assoc} on the identity of the nitronate and ammonium ion is also reasonable. The *K*_{assoc} values are summarized in Table VIII (70% Me₂SO) and Table IX (90% Me₂SO). *K*_{assoc} is seen to be higher for the more basic nitromethane anion than for phenylnitromethane anion (e.g., in 90% Me₂SO, *K*_{assoc} with morpholinium ion is 7.96 × 10² M⁻¹ for CH₂=NO₂⁻, 35.4 M⁻¹ for PhCH=NO₂⁻; *K*_{assoc} with 2-methoxyethylammonium ion is 60.1 M⁻¹ for CH₂=NO₂⁻, 9.33 M⁻¹ for PhCH=NO₂⁻). Likewise, *K*_{assoc} increases with the acidity of the ammonium ion within a family of ammonium ions (e.g., in 90% Me₂SO for PhCH=NO₂⁻, *K*_{assoc} = 9.33 M⁻¹ and 91.0 M⁻¹ for CH₃OCH₂CH₂NH₃⁺ and EtOOCCH₂NH₃⁺, respectively; or *K*_{assoc} = 3.23 M⁻¹ and 35.4 M⁻¹ for pipH⁺ and morH⁺, respectively; see also Figure 7). On the other hand, it is surprising that *K*_{assoc} = 10.6 for *n*-BuNH₃⁺/PhCH=NO₂⁻ in 90% Me₂SO is roughly the same as for CH₃OCH₂CH₂NH₃⁺/PhCH=NO₂⁻ (9.33), despite the higher p*K*_a^{BH} for *n*-BuNH₃⁺, and that *K*_{assoc} for pipH⁺/CH₂=NO₂⁻ and morH⁺/CH₂=NO₂⁻ in 70% Me₂SO are about the same. We believe that these inconsistencies are artifacts caused by large uncertainties in the *K*_{assoc} values for systems where *K*_{assoc} is small due to low acidity of the ammonium ion (*n*-BuNH₃⁺, pipH⁺) and/or a solvent in which *K*_{assoc} is inherently small (70% Me₂SO). The problem is that low *K*_{assoc} values lead only to modest downward curvature in the *k*_{obsd} vs ammonium concentration plots and this renders the determination of *K*_{assoc} uncertain. In our subsequent discussion we shall therefore omit *K*_{assoc} values that were calculated on the basis of weak curvature from further consideration of quantitative effects (values in parentheses in Tables VIII and IX).

One interesting result which is probably not an artifact is that *K*_{assoc} for CH₂=NO₂⁻ with secondary ammonium ions is higher than with primary ammonium ions at a given p*K*_a^{BH}, but the same phenomenon is not observed with PhCH=NO₂⁻ (Figure 7). A possible interpretation of these findings is that with primary ammonium ions the strength of the complex with CH₂=NO₂⁻ is weakened because one of the ammonio protons forms a hydrogen bond to the solvent (4). With the bulkier PhCH=NO₂⁻, this factor



(22) Jencks, W. P.; Brant, S. R.; Gandler, J. R.; Fendrich, G.; Nakamura, C. J. Am. Chem. Soc. 1982, 104, 7045.

may be counteracted by a steric effect, which could either reduce K_{assoc} with the *secondary* ammonium ions or hinder the approach of Me_2SO in 4 when $\text{R} = \text{Ph}$.

It is noteworthy that no association of the nitronate ions with carboxylic acids was detected. There are probably two reasons for this. The first is that for a given $\text{p}K_{\text{a}}^{\text{BH}}$, K_{assoc} with a carboxylic acid is likely to be smaller than with an ammonium ion because it does not benefit from the electrostatic attraction in the latter. The second is that the pH values required to study protonation of the nitronate ions by the carboxylic acids were rather low, which renders the $a_{\text{H}^+}/K_{\text{a}}^{\text{NOH}}$ term in eq 13 larger than the $K_{\text{assoc}}[\text{BH}^+]$ term, thus precluding the observation of curvature in the buffer plots. For example, with cyanoacetic acid ($\text{p}K_{\text{a}}^{\text{BH}} = 6.25$) studied at pH 6.25 (Table S4), one calculates $a_{\text{H}^+}/K_{\text{a}}^{\text{NOH}} = 30.2$. If K_{assoc} were one-tenth as high as for the similarly acidic cyanomethyl ammonium ion ($\text{p}K_{\text{a}}^{\text{BH}} = 5.94$), i.e., $K_{\text{assoc}} = 76 \text{ M}^{-1}$, the $K_{\text{assoc}}[\text{BH}^+]$ term at the highest $[\text{BH}^+]$ used (0.06 M) would only be 4.6, and curvature would not be detectable.

Application of the Hine Equation for Hydrogen-Bonded Complexes. Hine²³ has developed an equation that relates the association equilibrium constants of hydrogen-bonded complexes to the $\text{p}K_{\text{a}}$ of the donor, acceptor, solvent, and solvated proton. Jencks's version¹⁴ applied to our system is shown in eq 17. The interaction

$$\log K_{\text{assoc}} = \tau(\text{p}K_{\text{a}}^{\text{BH}} - \text{p}K_{\text{a}}^{\text{H}_2\text{O}})(\text{p}K_{\text{a}}^{\text{H}_3\text{O}^+} - \text{p}K_{\text{a}}^{\text{NOH}}) - \log 2[\text{H}_2\text{O}] \quad (17)$$

coefficient τ was estimated by Hine to be 0.024 in methanol and by Funderburk and Jencks²⁴ to be 0.013 in water. Recently Stahl and Jencks¹⁴ determined $\tau = 0.013$ experimentally by measuring the association between protonated amines and substituted phenolate ions in aqueous solution.

Application of eq 17 to our results in 90% Me_2SO affords the τ values summarized in Table IX, last column. There is some scatter in these values, but it is clear that they are much larger than 0.013: for $\text{CH}_2=\text{NO}_2^-$ the average τ value with primary ammonium ions is 0.031 ± 0.002 , with secondary ammonium ions 0.038 ± 0.001 ; for $\text{PhCH}=\text{NO}_2^-$ the average τ value for all ammonium ions (but excluding the values in parentheses due to large experimental error) is 0.028 ± 0.004 . The much higher τ values in our systems are of course a direct reflection of the much higher K_{assoc} values ($\sim 10 \text{ M}^{-1}$ to almost 10^3 M^{-1}) than those reported by Stahl and Jencks¹⁴ ($< 1 \text{ M}^{-1}$).

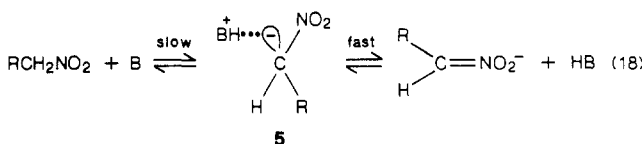
The major reason for the much larger τ values in our systems is undoubtedly the change in solvent. Hydrogen bonding to the nitronate ions by the solvent must be relatively weak in 90% Me_2SO , and the superior hydrogen bond acceptor ability of Me_2SO ²⁵ is not able to adequately compensate for this factor.

Similar increases in the equilibrium constant (and thus in τ) of hydrogen-bonded complexes with increasing Me_2SO content of the solvent have been reported. For example, the association equilibrium constant for phenols with their conjugate phenolate ion are of the order of 5 M^{-1} in 70% Me_2SO ,²⁶ $10\text{--}20 \text{ M}^{-1}$ in 80% Me_2SO ,²⁷ and $1500\text{--}2500 \text{ M}^{-1}$ in 100% Me_2SO .²⁸

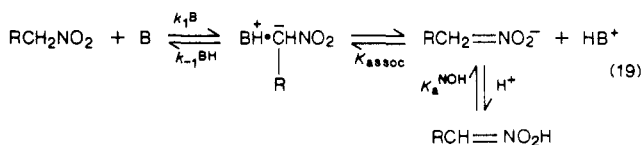
The high negative charge density on the nitronate ion oxygens compared to that on phenolate ions (Stahl and Jencks) probably constitutes an additional factor that enhances τ and K_{assoc} . The absence of curvature in the buffer plots of the reaction of acetylacetonate ion with protonated amines over the same concentration range and in the same solvent,^{11a} which implies much smaller K_{assoc} values than in the nitronate ion reactions, is consistent with this notion since the acetylacetonate ion has a much lower negative charge density on the oxygens.

One might have expected that, along with the higher negative charge density, the presence of two vicinal oxygens in the nitronate ion, both able to accept a hydrogen bond as shown in 4, would be an additional factor in enhancing K_{assoc} . However, if this factor were important, one would expect K_{assoc} for tertiary ammonium ions to be smaller than for primary and secondary ones since only one hydrogen bond is possible. This expectation is inconsistent with the fact that K_{assoc} for DabcoH^+ lies on the same Brønsted line as the primary and secondary ammonium ions (Figure 7) and has the same τ value.

Could the Hydrogen-Bonded Complex Represent Bordwell's Intermediate? Throughout our discussion it was assumed that the association complexes have a structure such as 1 or 4, i.e., there is hydrogen bonding of the ammonium ion to the oxygens of the nitronate ion. In this section we examine the question whether alternatively the association complexes could represent hydrogen bonding to carbon. Bordwell^{2,29} has suggested that the highly anomalous Brønsted α_{CH} values in the deprotonation of aryl nitroalkanes are not merely the consequence of a highly imbalanced transition state (charge delocalization into the nitro group and solvation lagging behind proton transfer) but may be due to the formation of a hydrogen-bonded (to carbon) intermediate (5) as shown in eq 18.



If the curvature in our buffer plots were indeed caused by an accumulation of 5 rather than 1, the reaction scheme shown in eq 12 would become



From the point of view of the rate equation, this scheme is indistinguishable from eq 12, with k_{obsd} given by eq 20.

$$k_{\text{obsd}} = k_1^{\text{B}}[\text{B}] + \frac{k_{-1}^{\text{BH}}K_{\text{assoc}}[\text{BH}]}{1 + \frac{a_{\text{H}^+}}{K_{\text{a}}^{\text{NOH}}} + K_{\text{assoc}}[\text{BH}]} \quad (20)$$

An analysis of our data according to eq 20 affords the same K_{assoc} values as analysis according to eq 13, and hence eq 19 cannot be refuted on the basis of the rate equation. Nevertheless, the notion that the curvature in our buffer plots (Figures 2–4) could be due to accumulation of 5 is unattractive. It is generally agreed that nitronate ions derive a large portion of their stabilization from the de-

(23) Hine, J. *J. Am. Chem. Soc.* **1972**, *94*, 5766.

(24) Funderburk, L. H.; Jencks, W. P. *J. Am. Chem. Soc.* **1978**, *100*, 6708.

(25) Taft, R. W.; Gurka, D.; Joris, L.; Schleyer, P. v. R.; Rakshys, J. *J. Am. Chem. Soc.* **1969**, *91*, 4801.

(26) Hibbert, F.; Robbins, H. J. *J. Am. Chem. Soc.* **1978**, *100*, 8238.

(27) Sorkhabi, H. A.; Hallé, J. C.; Terrier, F. *J. Chem. Res., Synop.* **1978**, 108 and 196.

(28) Bordwell, F. G.; McCallum, R. J.; Olmstead, W. N. *J. Org. Chem.* **1984**, *49*, 1424.

(29) Bordwell, F. G.; Hughes, D. L. *J. Am. Chem. Soc.* **1985**, *107*, 4737.

localization of the negative charge into the oxygens coupled with hydrogen-bonding solvation of this charge. Hydrogen bonding to carbon is notoriously weaker than to more electronegative atoms; it would not be able to compensate for the loss of delocalization and the hydrogen bonding to oxygen and render **5** more stable than **1**.

It should be noted though that exclusion of **5** as the association complex observed in this study does not refute Bordwell's hypothesis that **5** could be an intermediate (nonaccumulating) in the reaction. Saunder's³⁰ ¹⁴C kinetic isotope effect study does, however, argue strongly against **5** as a discrete intermediate.

Experimental Section

Materials. Phenylnitromethane was prepared from benzyl bromide and sodium nitrite by the procedure of Fukuyama et al.¹ Nitromethane and 1-chloro-2,4-dinitrobenzene were commercial products (Aldrich). Acetylacetone was available from a previous study.^{11a} The purification of the amines and carboxylic acids has been described in a previous paper.^{11a} Me₂SO was stored over 4-Å molecular sieves prior to use.

Reaction Solutions. The solutions were prepared essentially as described before.^{11a} For the 50% Me₂SO solutions, appropriate amounts of aqueous stock solutions were added to the Me₂SO and the volumetric flasks were topped off with water. For the 70% and 90% Me₂SO solutions, Me₂SO was added to the aqueous phase and the flasks were topped off with Me₂SO. Nitromethane and phenylnitromethane were introduced by injecting a few microliters of concentrated stock solutions in Me₂SO. pH measurements were performed as described previously.^{11a}

pK_a^{CH} Measurements. pK_a^{CH} of phenylnitromethane was determined by classical spectrophotometric procedures in all solvents. The same method could be used for nitromethane in water and in 50% Me₂SO. In 70% and 90% Me₂SO, the pK_a values are so high that it was difficult to measure accurate pH values due to sluggish response of the glass electrode. Instead, a method was chosen whereby nitromethane was used as the buffer and phenoxide ion (in 70% Me₂SO) or *p*-chlorophenoxide ion (in 90% Me₂SO) as an indicator. For example, in 90% Me₂SO, an indicator concentration of 8 × 10⁻⁵ M *p*-chlorophenol was used

with [CH₃NO₂] + [CH₂=NO₂⁻] = 0.004 M. From the known ε = 3300 M⁻¹ cm⁻¹ of *p*-chlorophenoxide ion at λ_{max} = 313.5 nm and its known pK_a = 13.86³¹ in 90% Me₂SO, the pH value of the solution could be deduced for various [CH₃NO₂]:[CH₂=NO₂⁻] ratios and hence pK_a^{CH} calculated. The procedure in 70% Me₂SO was analogous.

Rate Measurements. All kinetic determinations were performed in a Durrum-Gibson stopped-flow apparatus with computerized data acquisition.³² For reactions at pH > pK_a^{CH}, the nitroalkane was placed in a 10⁻³ M HCl solution of appropriate ionic strength and then mixed in the stopped-flow apparatus with the amine buffer or KOH solution. For reactions at pH < pK_a^{CH}, the nitroalkane was placed in a 10⁻³ M KOH solution and then mixed in the stopped-flow apparatus with the carboxylic or amine buffer or HCl solution. Due to gradual decomposition of the basic nitroalkane solution, particularly nitromethane, the stopped-flow experiments were executed immediately after preparing the solutions. In the experiments where formation of the nitronic acid was unimportant, the reactions were monitored at or near λ_{max} of the nitronate ion (for CH₂=NO₂⁻, λ_{max} = 233 nm (ε 8400) in water, 248 nm (ε 5900) in 50% Me₂SO, and 258 nm (ε 6400) in 90% Me₂SO; for PhCH=NO₂⁻, λ_{max} = 289 nm (ε 21 400) in water, 303 nm (ε 20 800) in 50% Me₂SO, and 326 nm (ε 22 300) in 90% Me₂SO). In those situations where phenylnitromethane nitronic acid (aci form) formation was extensive, the kinetic experiments were performed at λ_{max} of this latter (286 nm in 90% Me₂SO). This was not possible with nitromethane, though, because λ_{max} of CH₂=NO₂H is buried in the Me₂SO absorption, and hence kinetic measurements with strongly acidic buffers could not be carried out.

Acknowledgment. This research was supported by Grant CHE-8617370 from the National Science Foundation and by the donors of the Petroleum Research Fund, administered by the American Chemical Society (Grant No. 17991-AC4).

Supplementary Material Available: Kinetic data, Tables S1-12 (18 pages). Ordering information is given on any current masthead page.

(31) Hallé, J.-C.; Gaboriaud, R.; Schaal, R. *Bull. Soc. Chim. Fr.* 1970, 2047.

(32) Software developed by F. A. Brand.

(30) Wilson, J. C.; Källsson, I.; Saunders, W. H., Jr. *J. Am. Chem. Soc.* 1980, 102, 4780.

Notes

A New Synthesis of Pentasubstituted Benzenes by Tandem Dimerization-Ring Opening of 3-Halo-2,5-dialkylthiophene 1,1-Dioxides

Salo Gronowitz,* Grigorios Nikitidis, Anders Hallberg, and Rolf Servin

Division of Organic Chemistry 1, Chemical Center, University of Lund, P.O. Box 124, S-221 00 Lund, Sweden

Received December 17, 1987

We have recently studied the reactions of a series of 3-halo-2,5-dialkylthiophene 1,1-dioxides with various nucleophiles. We found, for example, that the reaction with secondary amines in toluene offered an excellent stereoselective route to one of the four possible dialkylamino-methyl-substituted halobutadienes.¹

We have also studied the reaction with benzylthiolate and with various alkoxides.² In this connection, we treated 3-bromo-2,5-dimethylthiophene 1,1-dioxide with sodium *tert*-butoxide in *tert*-butyl alcohol. Instead of obtaining the addition products obtained with sodium ethoxide and sodium benzyl oxide, a crystalline compound, mp 63-63.5 °C, analyzed correctly as C₁₂H₁₃Br was isolated. The yield of this product was increased by omitting the *tert*-butoxide and refluxing the *tert*-butyl alcohol solution for a longer period (120 h). The IR spectrum showed a weak band at 2230 cm⁻¹, indicating the presence of a disubstituted acetylene.

Its ¹H and ¹³C NMR spectra indicated the presence of four nonequivalent methyl groups and one aromatic pro-

(1) Gronowitz, S.; Hallberg, A.; Nikitidis, G. *Tetrahedron* 1987, 43, 4793.

(2) Gronowitz, S.; Nikitidis, G.; Hallberg, A. *Chem. Scr.*, in press.